

FAST MISSING-DATA IAA BY LOW RANK COMPLETION

Johan Karlsson*, William Rowe*, Luzhou Xu*, George Glentis†, and Jian Li*

* University of Florida, Department of Electrical and Computer Engineering

† University of Peloponnese, Department of Science and Technology of Telecommunications

ABSTRACT

The adaptive spectral estimation method IAA provides better performance than the periodogram at the cost of higher computational complexity. Current fast IAA algorithms reduce the computational complexity using Toeplitz/Vandermonde structures, but are not efficient for missing data cases when the number of missing samples is small. We considerably reduce the computational complexity compared to the state-of-the-art by using a low rank completion to transform the problem to a Toeplitz/Vandermonde structured problem.

1. INTRODUCTION

A fundamental task in spectral estimation is to estimate noisy sinusoids' frequencies and amplitudes from a set of measurements [1]. The common solution is to use the periodogram to estimate the spectra, a method which in general suffers from large sidelobes and poor resolution. In the case of missing data, the sidelobe problem becomes even worse due to modulation in the sampling domain by the incomplete sampling pattern.

A recently developed high resolution nonparametric spectral estimation technique, the iterative adaptive approach (IAA) [2], can also be used in the missing data case (MIAA) [3]. This is a method based on iterative weighted minimization, where the weight is updated to increase the resolution and suppress sidelobes. IAA provides resolution superior to the periodogram, and has the advantage that only a single snapshot is required. The major drawback of IAA is the computational costs for a direct implementation. In two recent papers ([4], [5]) implementations of IAA were developed based on FFT operations, which considerably speeds up the algorithm and makes it applicable for larger problems. These fast implementations utilize Toeplitz and Vandermonde structures that arise when the sampling grid is uniform and

complete. When the sampling grid is not complete the structures are lost, and the fast implementations are not efficient when the number of missing samples is small. To resolve this, we use a low rank completion to transform the problem to the structured problem where the covariance matrix is Toeplitz. This leads to the main contribution of this paper, a fast implementation of MIAA which is considerably faster than the state-of-the-art for the case when the proportion of missing data is small.

In Section 2 we set up the data model, discuss the spectral estimation problem, introduce the algorithm IAA, and discuss the computational complexity. In Section 3 the missing data algorithm is discussed and we present the new fast algorithm for missing data IAA. In Section 4 we present examples that illustrate the computational benefits of the new algorithms.

2. SPECTRAL ESTIMATION AND IAA

Consider the problem of recovering the spectral content from a measured signal. Let $\mathbf{y} = [y_0, y_1, \dots, y_{N-1}]^T$ denote a sampled data sequence of length N and let

$$\mathbf{A} = [\mathbf{a}(\omega_0), \dots, \mathbf{a}(\omega_{K-1})] \quad (1)$$

be an oversampled Fourier matrix such that $K > N$. The columns of \mathbf{A} are $\mathbf{a}(\omega_k) = [1, e^{j\omega_k}, \dots, e^{j(N-1)\omega_k}]^T$ which correspond to the frequency vectors and ω_k corresponds to the frequency grid point $\omega_k = \frac{2\pi k}{K}$, for $k = 0, \dots, K-1$. Let $\mathbf{x} = [x_0, x_1, \dots, x_{K-1}]^T$ where x_k denotes the complex spectral content at frequency ω_k of the signal \mathbf{y} . The goal is to estimate an envelop for \mathbf{x} from the data model

$$\mathbf{y} = \mathbf{A}\mathbf{x} + \mathbf{e}, \quad (2)$$

where \mathbf{e} is the noise. The most common method for solving this is the periodogram (matched filter method),

$$x_k = \frac{\mathbf{a}(\omega_k)^* \mathbf{y}}{\mathbf{a}(\omega_k)^* \mathbf{a}(\omega_k)}, \quad k = 0, 1, \dots, K-1, \quad (3)$$

which corresponds to time domain convolution of the signal \mathbf{y} with the column vectors in \mathbf{A} . This is computationally efficient, but suffers from high sidelobes and poor resolution. One way to overcome these issues is to use data-adaptive

This work was supported in part by Swedish Research Council, NSF CCF-1218388, and the Department of Defense. The views and conclusions contained herein are those of the authors and should not be interpreted as necessarily representing the official policies or endorsements, either expressed or implied, of the U.S. Government. The U.S. Government is authorized to reproduce and distribute reprints for Governmental purposes notwithstanding any copyright notation thereon. L. Xu and J. Li are also affiliated with the IAA, Inc. Email: {jkarlsson, wrowe001}@ufl.edu, {xuluzhou, li}@dsp.ufl.edu, gglentis@uop.gr.

methods such as the Capon method [6], [7], Amplitude and Phase Estimation (APES) [8], [9], or Iterative Adaptive Approach (IAA) [2]. Here we will focus explicitly on IAA as it has shown promise in the fields of radar imaging, sonar, communications [2], medical diagnostics [10], information forensics [11], and general spectral estimation [12].

2.1. Iterative Adaptive Approach (IAA)

IAA seeks to find a spectral estimate x_k in (2) by modeling the rest of the spectrum x_ℓ , $\ell \neq k$, as interference [2]. The covariance matrix \mathbf{Q}_k of the interference and noise, where interference refers to all the signals at frequency grid points other than the grid point of interest ω_k , is given by

$$\mathbf{Q}_k = \mathbf{R} - p_k \mathbf{a}(\omega_k) \mathbf{a}(\omega_k)^*,$$

where

$$\mathbf{R} = \sum_{k=0}^{K-1} p_k \mathbf{a}(\omega_k) \mathbf{a}(\omega_k)^* = \mathbf{A} \mathbf{P} \mathbf{A}^*. \quad (4)$$

Here \mathbf{R} is the covariance matrix of the data and $\mathbf{P} = \text{diag}(\mathbf{p})$, where $\mathbf{p} = (p_0, p_1, \dots, p_{K-1})^T$, and $p_k = |x_k|^2$ denotes the power estimate at the frequency grid point ω_k , for $k = 0, 1, \dots, K-1$. This results in minimization of the weighted quadratic cost function

$$(\mathbf{y} - \mathbf{a}(\omega_k) x_k)^* \mathbf{Q}_k^{-1} (\mathbf{y} - \mathbf{a}(\omega_k) x_k), \quad (5)$$

where the optimal solution is given by

$$x_k = \frac{\mathbf{a}(\omega_k)^* \mathbf{Q}_k^{-1} \mathbf{y}}{\mathbf{a}(\omega_k)^* \mathbf{Q}_k^{-1} \mathbf{a}(\omega_k)} = \frac{\mathbf{a}(\omega_k)^* \mathbf{R}^{-1} \mathbf{y}}{\mathbf{a}(\omega_k)^* \mathbf{R}^{-1} \mathbf{a}(\omega_k)}, \quad (6)$$

for $k = 0, 1, \dots, K-1$. The second equality in (6) is obtained using the matrix inversion lemma. This considerably speeds up the calculation since inversion of \mathbf{Q}_k is not needed for each frequency grid point. Note that \mathbf{R} depends on \mathbf{x} , hence solving Equations (4) and (6) is a non-trivial task. IAA handles this in an iterative manner. The algorithm starts with an initial solution which is often taken as the Periodogram (3), or equivalently letting $\mathbf{R} = \mathbf{I}$. The following steps are then taken:

1. The covariance matrix \mathbf{R} is calculated using (4),
2. x_k is calculated using (6) for $k = 0, 1, \dots, K-1$.

Steps 1) and 2) are repeated until convergence, and the spectral estimate in the point ω_k is given by $p_k = |x_k|^2$. From empirical results usually 10 – 15 iterations are sufficient for the algorithm to converge [2].

2.2. Computational complexities and fast IAA

In each iteration IAA requires evaluation of the numerator and denominator of the expression (6), denoted by

$$\Phi_N(\omega) = \mathbf{a}(\omega)^* \mathbf{R}^{-1} \mathbf{y}, \quad (7)$$

$$\Phi_D(\omega) = \mathbf{a}(\omega)^* \mathbf{R}^{-1} \mathbf{a}(\omega), \quad (8)$$

at each of the points ω_k , $k = 0, 1, \dots, K-1$. Using a brute force approach, this takes $\mathcal{O}(N^2 K)$ [13] which is too computationally demanding in many applications. In [4] an algorithm is developed where Toeplitz and Vandermonde structures are used to calculate IAA several orders of magnitudes quicker by utilizing FFT operations [14, 15]. The overall computational cost is $\mathcal{O}(N^2 + K \log K)$. Here the Levinson-Durbin (LD) algorithm is used for finding the solution to the Gohberg-Semencul (GS) factorization of \mathbf{R} (see, e.g., [16, 1]). This methodology for computing fast IAA was independently developed in [4] and [5], and they are based on earlier fast implementations of APES [17].

3. MISSING DATA IAA AND FAST CALCULATIONS

In [3], IAA was applied to problems where data samples are missing.¹ In this section we treat the spectral estimation part of missing data IAA and provide a new algorithm that is fast when the number of missing data samples is small.

Consider the problem of estimating \mathbf{x} from a vector of available data \mathbf{y}_g , which is a subset of the full data vector \mathbf{y} . The available and missing part of \mathbf{y} may be represented as $\mathbf{y}_g = \mathbf{S}_g \mathbf{y}$, $\mathbf{y}_m = \mathbf{S}_m \mathbf{y}$, where $\mathbf{S}_g \in \mathbb{R}^{N_g \times N}$ and $\mathbf{S}_m \in \mathbb{R}^{N_m \times N}$ are the selection matrices corresponding to the available and missing samples, respectively. Here N_g and N_m denote the number of available data and missing data, and hence $N = N_g + N_m$.

The data model (2) is now replaced by

$$\mathbf{y}_g = \mathbf{S}_g \mathbf{y} = \mathbf{S}_g \mathbf{A} \mathbf{x} + \mathbf{e} \quad (9)$$

where $\mathbf{S}_g \mathbf{A}$ is the steering matrix and the vector \mathbf{x} is sought. Since IAA is applicable for the missing data case, each iteration of MIAA is now to evaluate

$$x_k = \frac{\mathbf{a}_g(\omega_k)^* \mathbf{R}_g^{-1} \mathbf{y}_g}{\mathbf{a}_g(\omega_k)^* \mathbf{R}_g^{-1} \mathbf{a}_g(\omega_k)}, \quad (10)$$

where $\mathbf{a}_g(\omega_k) = \mathbf{S}_g \mathbf{a}(\omega_k)$,

$$\mathbf{R}_g = \mathbf{S}_g \mathbf{A} \mathbf{P} \mathbf{A}^* \mathbf{S}_g^* = \mathbf{S}_g \mathbf{R} \mathbf{S}_g^*, \quad (11)$$

and as before $\mathbf{P} = \text{diag}(p_k)$ where $p_k = |x_k|^2$, for $k = 0, \dots, K-1$. Denote the numerator and denominator of (10) by

$$\begin{aligned} \Psi_N(\omega_k) &= \mathbf{a}_g(\omega_k)^* \mathbf{R}_g^{-1} \mathbf{y}_g \\ \Psi_D(\omega_k) &= \mathbf{a}_g(\omega_k)^* \mathbf{R}_g^{-1} \mathbf{a}_g(\omega_k). \end{aligned}$$

Here \mathbf{R}_g is not Toeplitz and several of the steps in the fast implementation from [4] breaks down, including the GS factorization. A fast approach was proposed in [5] requiring $\mathcal{O}(N_g^3 + K \log K)$ number of operations. The main burden here is the inversion of the matrix \mathbf{R}_g . If the number

¹This case may be seen as a problem with nonuniform data sampling, hence IAA still applies [3].

of available samples N_g is small, then this is not a problem. However, if the number of available samples N_g is large, then this inversion will be the bottleneck.

3.1. Fast calculation of missing data IAA

Consider the case where the number of missing samples N_m is small compared to all samples N . The problem is how to utilize the structure of \mathbf{R}_g and \mathbf{S}_g for evaluating the trigonometric polynomials $\Psi_N(\omega)$ and $\Psi_D(\omega)$. The calculations rely on the following key proposition, which allows us to express the matrix product $\mathbf{S}_g^* \mathbf{R}_g^{-1} \mathbf{S}_g$ as a sum of a low rank matrix and the inverse of a Toeplitz matrix.

Proposition 1 Let $\mathbf{R} > 0$ and \mathbf{R}_g be defined by (11) where \mathbf{A} is the steering matrix defined in (1). Then

$$\mathbf{S}_g^* \mathbf{R}_g^{-1} \mathbf{S}_g = \mathbf{R}^{-1} - \mathbf{\Gamma}$$

where $\mathbf{\Gamma}$ is given by

$$\mathbf{\Gamma} := \mathbf{R}^{-1} \mathbf{S}_m^* (\mathbf{S}_m \mathbf{R}^{-1} \mathbf{S}_m^*)^{-1} \mathbf{S}_m \mathbf{R}^{-1}.$$

Proof: Let \mathbf{S} denote the unitary matrix $\mathbf{S}^T = (\mathbf{S}_g^T, \mathbf{S}_m^T)$ which may be used to partition \mathbf{R} corresponding to the missing and available samples of \mathbf{y}

$$\begin{pmatrix} \mathbf{R}_g & \mathbf{R}_{gm} \\ \mathbf{R}_{mg} & \mathbf{R}_m \end{pmatrix} = \mathbf{S} \mathbf{R} \mathbf{S}^* = \begin{pmatrix} \mathbf{S}_g \mathbf{R} \mathbf{S}_g^* & \mathbf{S}_g \mathbf{R} \mathbf{S}_m^* \\ \mathbf{S}_m \mathbf{R} \mathbf{S}_g^* & \mathbf{S}_m \mathbf{R} \mathbf{S}_m^* \end{pmatrix}.$$

Since \mathbf{S} is unitary, we have $(\mathbf{S} \mathbf{R} \mathbf{S}^*)^{-1} = \mathbf{S} \mathbf{R}^{-1} \mathbf{S}^*$ and blockwise matrix inversion gives

$$\begin{aligned} \mathbf{R}_g^{-1} &= (\mathbf{S}_g \mathbf{R} \mathbf{S}_g^*)^{-1} \\ &= \mathbf{S}_g \mathbf{R}^{-1} \mathbf{S}_g^* - \mathbf{S}_g \mathbf{R}^{-1} \mathbf{S}_m^* (\mathbf{S}_m \mathbf{R}^{-1} \mathbf{S}_m^*)^{-1} \mathbf{S}_m \mathbf{R}^{-1} \mathbf{S}_g^* \\ &= \mathbf{S}_g (\mathbf{R}^{-1} - \mathbf{\Gamma}) \mathbf{S}_g^*. \end{aligned}$$

Note that $\mathbf{\Gamma} \mathbf{S}_m^* = \mathbf{R}^{-1} \mathbf{S}_m^*$, and hence

$$\begin{aligned} \mathbf{S}_g^* \mathbf{R}_g^{-1} \mathbf{S}_g &= \mathbf{S}_g^* \mathbf{S}_g (\mathbf{R}^{-1} - \mathbf{\Gamma}) \mathbf{S}_g^* \mathbf{S}_g \\ &= (\mathbf{I}_N - \mathbf{S}_m^* \mathbf{S}_m) (\mathbf{R}^{-1} - \mathbf{\Gamma}) (\mathbf{I}_N - \mathbf{S}_m^* \mathbf{S}_m) \\ &= \mathbf{R}^{-1} - \mathbf{\Gamma}. \end{aligned} \quad \square$$

Denote by $\mathbf{y}_f = \mathbf{S}_g^* \mathbf{y}_g$, the vector \mathbf{y} with the missing samples zeroed out. Using Proposition 1, we can express the numerator $\Psi_N(\omega)$ and denominator $\Psi_D(\omega)$ in terms of the full data numerator $\Phi_N(\omega)$ and denominator $\Phi_D(\omega)$:

$$\begin{aligned} \Psi_N(\omega) &= \mathbf{a}(\omega)^* \mathbf{S}_g^* \mathbf{R}_g^{-1} \mathbf{S}_g \mathbf{y}_f = \mathbf{a}(\omega)^* (\mathbf{R}^{-1} - \mathbf{\Gamma}) \mathbf{y}_f \\ &= \Phi_N(\omega) - \mathbf{a}(\omega)^* \mathbf{\Gamma} \mathbf{y}_f, \end{aligned} \quad (12)$$

$$\begin{aligned} \Psi_D(\omega) &= \mathbf{a}(\omega)^* \mathbf{S}_g^* \mathbf{R}_g^{-1} \mathbf{S}_g \mathbf{a}(\omega) = \mathbf{a}(\omega)^* (\mathbf{R}^{-1} - \mathbf{\Gamma}) \mathbf{a}(\omega) \\ &= \Phi_D(\omega) - \mathbf{a}(\omega)^* \mathbf{\Gamma} \mathbf{a}(\omega). \end{aligned} \quad (13)$$

Here Φ_N and Φ_D may be evaluated efficiently as in [4] where \mathbf{y}_f replaces \mathbf{y} , using the Toeplitz structure of \mathbf{R} . The rank of $\mathbf{\Gamma}$ is equal to N_g , a fact which may be used for calculating the remaining parts of Ψ_N and Ψ_D . Next we will utilize this structure in order to evaluate (12) and (13) efficiently.

3.1.1. Get \mathbf{R} , the GS factorization of \mathbf{R}^{-1} , and evaluate $\Phi_N(\omega)$ and $\Phi_D(\omega)$

This is done exactly as in [4] using $\mathbf{y} = \mathbf{y}_f$ in $\mathcal{O}(N^2 + K \log K)$.

3.1.2. Get $\mathbf{L} = (\mathbf{S}_m \mathbf{R}^{-1} \mathbf{S}_m^*)^{-1/2}$ and $\mathbf{X} = \mathbf{\Gamma}^{1/2}$

Calculate $\mathbf{R}^{-1} = [\mathbf{r}_1^{\text{inv}}, \dots, \mathbf{r}_N^{\text{inv}}]$ recursively using the displacement structure of \mathbf{R}^{-1} (see (18)-(20) in [18])

$$\mathbf{r}_k^{\text{inv}} = \begin{cases} (\mathbf{u} \mathbf{u}^* - \tilde{\mathbf{u}} \tilde{\mathbf{u}}^*) \mathbf{e}_k / u(1) & k = 1 \\ \mathbf{D} \mathbf{r}_{k-1}^{\text{inv}} + (\mathbf{u} \mathbf{u}^* - \tilde{\mathbf{u}} \tilde{\mathbf{u}}^*) \mathbf{e}_k / u(1) & k > 1, \end{cases}$$

in $\mathcal{O}(N^2)$. Here $\mathbf{R} \mathbf{u} = \mathbf{e}_1$, $\tilde{\mathbf{u}}^* = (0, u(N), u(N-1), \dots, u(2))$ and \mathbf{D} is the shift (down) matrix. Then get $\mathbf{S}_m \mathbf{R}^{-1} \mathbf{S}_m^*$ by selecting the rows and columns corresponding to the missing data. Let $\mathbf{L} \in \mathbb{C}^{N_m \times N_m}$ be the inverse of the Cholesky factor of $\mathbf{S}_m \mathbf{R}^{-1} \mathbf{S}_m^*$ (calculated in $\mathcal{O}(N_m^3)$), i.e.,

$$\mathbf{L} \mathbf{L}^* = (\mathbf{S}_m \mathbf{R}^{-1} \mathbf{S}_m^*)^{-1}.$$

Finally, get $\mathbf{X} \in \mathbb{C}^{N \times N_m}$ satisfying $\mathbf{X} \mathbf{X}^* = \mathbf{\Gamma}$, by multiplication $\mathbf{X} = \mathbf{R}^{-1} (\mathbf{S}_m^* \mathbf{L})$ using² the GS factorization of \mathbf{R}^{-1} , in $\mathcal{O}(N_m N \log N)$.

3.1.3. Evaluate $\mathbf{a}(\omega)^* \mathbf{\Gamma} \mathbf{y}_f$

The remaining part of the numerator Ψ_N , i.e., $\mathbf{a}(\omega)^* \mathbf{\Gamma} \mathbf{y}_f$, may be calculated by noting that

$$\mathbf{a}(\omega)^* \mathbf{\Gamma} \mathbf{y}_f = \mathbf{a}(\omega)^* \mathbf{X} \mathbf{L}^* \mathbf{S}_m \mathbf{R}^{-1} \mathbf{y}_f. \quad (14)$$

In this expression first the $\mathbf{R}^{-1} \mathbf{y}_f$ multiplication is carried out using the GS-factorization, $\mathbf{S}_m (\mathbf{R}^{-1} \mathbf{y}_f)$ by selecting the rows corresponding to the missing data, and then $\mathbf{X} \mathbf{L}^* (\mathbf{S}_m \mathbf{R}^{-1} \mathbf{y}_f)$ by standard matrix-vector calculations (in $\mathcal{O}(N_g N + N \log N)$). Finally (14) is evaluated at ω_k for $k = 0, 1, \dots, K-1$ by noting that³

$$[\mathbf{a}(\omega_0)^* \mathbf{\Gamma} \mathbf{y}_f, \dots, \mathbf{a}(\omega_{K-1})^* \mathbf{\Gamma} \mathbf{y}_f]^T = \mathcal{F}(\mathbf{X} \mathbf{L}^* \mathbf{S}_m \mathbf{R}^{-1} \mathbf{y}_f)_K.$$

3.1.4. Evaluate $\mathbf{a}(\omega)^* \mathbf{\Gamma} \mathbf{a}(\omega)$

The remaining part of the numerator, i.e., $\mathbf{a}(\omega)^* \mathbf{\Gamma} \mathbf{a}(\omega)$ may be calculated by noting that

$$\mathbf{a}(\omega)^* \mathbf{\Gamma} \mathbf{a}(\omega) = \mathbf{a}(\omega)^* \mathbf{X} \mathbf{X}^* \mathbf{a}(\omega) = \sum_{\ell=-N+1}^{N-1} c_\ell e^{j\ell\omega}$$

is a trigonometric polynomial. Here the coefficient c_ℓ is the ℓ th diagonal of $\mathbf{X} \mathbf{X}^*$ ($c_\ell = \bar{c}_{-\ell}$), and may be calculated in

²For small data sizes, multiplication $(\mathbf{R}^{-1} \mathbf{S}_m^*) \mathbf{L}$ is faster $\mathcal{O}(N_m^2 N)$.

³A fast Fourier transform operation (FFT) of size F is denoted by $\mathcal{F}(\cdot)_F$, where appropriate zero padding is performed if necessary. A denotation of $(\cdot)_{1:N}$ represents an indexing operation, i.e. elements 1 to N of a vector.

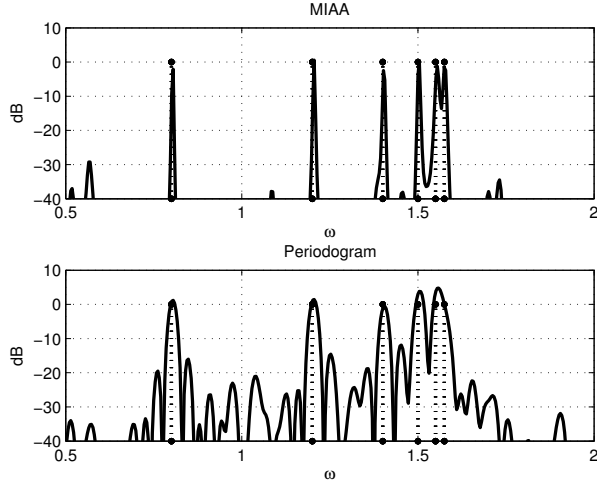


Fig. 1. Upper graph: missing data IAA spectral estimate. Lower graph: periodogram based on the available data.

$\mathcal{O}(N_m N \log N)$ using Toeplitz matrices (c.f., Appendix B [19])

$$\begin{pmatrix} c_{N-1} \\ \vdots \\ c_0 \end{pmatrix} = \sum_{\ell=1}^{N_m} \begin{pmatrix} \mathbf{X}(1, \ell) \\ \vdots \\ \mathbf{X}(N, \ell) \end{pmatrix} \begin{pmatrix} \overline{\mathbf{X}(N, \ell)} \\ \vdots \\ \overline{\mathbf{X}(1, \ell)} \end{pmatrix}.$$

Since the grid $\{\omega_k\}_{k=0}^{K-1}$ is uniform, $\mathbf{a}(\omega_k)^* \mathbf{\Gamma} \mathbf{a}(\omega_k)$ may be computed using FFT from the coefficients $\{c_n\}_{n=-N+1}^{N-1}$. This may be expressed as

$$\phi_{\mathbf{\Gamma}} = \mathcal{F}(\mathbf{c}) \quad (15)$$

where $\mathbf{c} = [c_0, c_1, \dots, c_{N-1}, \mathbf{0}_{K-2N+1}^T, c_{-N+1}, \dots, c_{-1}]^T$ and $\phi_{\mathbf{\Gamma}} = [\mathbf{a}(\omega_0)^* \mathbf{\Gamma} \mathbf{a}(\omega_0), \dots, \mathbf{a}(\omega_{K-1})^* \mathbf{\Gamma} \mathbf{a}(\omega_{K-1})]^T$, which is evaluated in $\mathcal{O}(K \log K)$.

3.1.5. Get $\Psi_N(\omega)$ and $\Psi_D(\omega)$

Get the evaluations of $\Psi_N(\omega)$ and $\Psi_D(\omega)$ from (12) and (13) using (14) and (15). Each iteration is calculated in $\mathcal{O}(N_m^3 + N_m N \log N + N^2 + K \log K)$.

4. APPLICATION: SINUSOID IDENTIFICATION

Consider an example of identification of sinusoids in noise where the signal y_n is given by

$$y_n = \sum_{\ell=1}^6 2 \sin(n\hat{\omega}_{\ell} + v_{\ell}) + w_n, \quad n = 0, 1, \dots, N-1,$$

where w_n is Gaussian white noise with variance 1, v_{ℓ} is a random variable with uniform distribution on $[0, 2\pi]$, and $\hat{\omega}_{\ell}$ denote the frequencies (0.8, 1.2, 1.4, 1.5, 1.55, 1.575) of the

real sinusoids. In the first example, $N = 200$, $K = 8N = 1600$ and 10% (= 20) of the samples are missing in two gaps. Spectral estimates are based on the missing data IAA and the periodogram.

Figure 1 shows the spectral estimates, where it can be seen that MIAA has considerably lower sidelobes and better resolution than the periodogram. In this work we focus on the computational complexity of MIAA, and refer to [13] and [3] for comparison of MIAA with other methods. Instead we compare the computational complexity of the proposed implementation of MIAA with the ones proposed in [5, 13].

Next consider the two cases $N \in \{2000, 8000\}$ and $K = 8N$. For each of those cases we compare the average time to perform a MIAA iteration over 10 total iterations of the proposed algorithm with the average time to invert \mathbf{R}_g in each iteration. This is done by selecting missing data randomly, with the missing data ratio going from 5% to 40%. The results are shown in Table 1, and when the missing data is less than 25%, the proposed algorithm provides significant reduction of the computation time compared to the state-of-the-art [5, 13].

Table 1. Average computation time per iteration

Missing data	$N = 2000, K = 8N$		$N = 8000, K = 8N$	
	MIAA	Invert \mathbf{R}_g	MIAA	Invert \mathbf{R}_g
5%	0.25	2.25	2.62	121.09
10%	0.31	2	4.17	104.09
15%	0.38	1.65	7.66	87.59
20%	0.48	1.41	13.98	73.06
25%	0.59	1.18	22.93	59.09
30%	0.75	0.99	35.95	48.41
35%	0.98	0.82	50.21	39.03
40%	1.34	0.67	71.66	31.17

5. CONCLUSIONS

In this paper a new approach for fast missing data IAA is designed for cases where the amount of missing data is small. This method utilizes structures in the MIAA algorithm and a low rank completion to replace a nonstructured problem with a structured problem. This allows for reducing the computational complexity from $\mathcal{O}((N - N_m)^3 + K \log K)$ to $\mathcal{O}(N_m^3 + N_m N \log N + N^2 + K \log K)$, which is a considerable improvement when the number of missing data N_m is much less than the total number of data N . The proposed method shows considerable improvements in computational complexity compared to the state-of-the-art [5, 13]. Asymptotically this implementation is faster whenever $N_m < N_g$, and from the examples there is considerable improvement in computation times for missing data ratios less than 25%.

6. REFERENCES

- [1] P. Stoica and R. L. Moses, *Spectral Analysis of Signals*. Upper Saddle River, NJ: Prentice-Hall, 2005.
- [2] T. Yardibi, J. Li, P. Stoica, M. Xue, and A. B. Baggeroer, "Source localization and sensing: A nonparametric iterative adaptive approach based on weighted least squares," *IEEE Transactions on Aerospace and Electronic Systems*, vol. 46, pp. 425 – 443, Jan. 2010.
- [3] P. Stoica, J. Li, and J. Ling, "Missing data recovery via a nonparametric iterative adaptive approach," *IEEE Signal Processing Letters*, vol. 16, pp. 241–244, April 2009.
- [4] M. Xue, L. Xu, and J. Li, "IAA spectral estimation: Fast implementation using the Gohberg-Semencul factorization," *IEEE Transactions on Signal Processing*, vol. 59, pp. 3251–3261, July 2011.
- [5] G.-O. Glentis and A. Jakobsson, "Efficient implementation of iterative adaptive approach spectral estimation techniques," *IEEE Transactions on Signal Processing*, vol. 59, pp. 4154–4167, September 2011.
- [6] J. Capon, "High resolution frequency-wavenumber spectrum analysis," *Proceedings of the IEEE*, vol. 57, pp. 1408–1418, August 1969.
- [7] R. T. Lacoss, "Data adaptive spectral analysis methods," *Geophysics*, vol. 36, pp. 661–675, August 1971.
- [8] J. Li and P. Stoica, "An adaptive filtering approach to spectral estimation and sar imaging," *IEEE Transactions on Signal Processing*, vol. 44, pp. 1469–1484, June 2009.
- [9] P. Stoica, H. Li, and J. Li, "A new derivation of the APES filter," *IEEE Signal Processing Letters*, vol. 6, pp. 205–206, August 1999.
- [10] A. Jakobsson, G. Glentis, and E. Gudmundson, "Computationally efficient time-recursive IAA-based blood velocity estimation," *IEEE Transactions on Signal Processing*, vol. 60, pp. 3853–3858, July 2012.
- [11] O. Ojowu, J. Karlsson, J. Li, and Y. Liu, "ENF extraction from digital recordings using adaptive techniques and frequency tracking," *IEEE Transactions on Information Forensics and Security*, vol. 7, pp. 1330–1338, August 2012.
- [12] P. Stoica, J. Li, and H. He, "Spectral analysis of non-uniformly sampled data: A new approach versus the periodogram," *IEEE Transactions on Signal Processing*, vol. 57, pp. 843–858, March 2009.
- [13] D. Vu, L. Xu, M. Xue, and J. Li, "Nonparametric missing sample spectral analysis and its applications to interrupted sar," *IEEE Journal of Selected Topics in Signal Processing*, vol. 6, pp. 1–14, February 2012.
- [14] R. Gray, *Toeplitz and circulant matrices: A review*. Foundations and Trends in Communications and Information Theory, 2006.
- [15] G. H. Golub and C. F. V. Loan, *Matrix Computations*. Baltimore, MD: Johns Hopkins University Press, 1989.
- [16] I. Gohberg and V. Olshevsky, "Circulants, displacements and decompositions of matrices," *Integral Equations and Operator Theory*, vol. 15, no. 5, pp. 730–743, 1992.
- [17] G. Glentis, "A fast algorithm for APES and Capon spectral estimation," *IEEE Transactions on Signal Processing*, vol. 56, pp. 4207–4220, September 2008.
- [18] J. Jensen, G. Glentis, M. Christiansen, A. Jakobsson, and S. Jensen, "Computationally efficient iaa-based estimation of the fundamental frequency," *Proc. 20th EUSIPCO*, August 2012.
- [19] E. Larsson and P. Stoica, "Fast implementation of two-dimensional APES and Capon spectral estimators," *Multidimensional Systems and Signal Processing*, vol. 13, pp. 35–54, January 2002.